Asian Journal of Physical and Chemical Sciences

2(4): 1-19, 2017; Article no.AJOPACS.35244
ISSN: 2456-7779

On Thermal Factor and MHD Mixed Convective Oscillatory Blood Flow in a Bifurcating Artery

W. I. A. Okuyade[1*] and T. M. Abbey[2]

[1]Department of Mathematics and Statistics, University of Port Harcourt, Port Harcourt, Nigeria.
[2]Applied Mathematics and Theoretical Physics Group, Department of Physics, University of Port Harcourt, Port Harcourt, Nigeria.

Authors' contributions

This work was carried out in collaboration between both authors. Both authors read and approved the final manuscript.

Article Information

DOI: 10.9734/AJOPACS/2017/35244
Editor(s):
(1) Shridhar N. Mathad, Department of Engineering Physics, K.L.E. Society's K.L.E. Institute of Technology, Gokul, Hubli, India.
Reviewers:
(1) John Abraham, University of St. Thomas, USA.
(2) Jagdish Prakash, University of Botswana, Botswana.
Complete Peer review History: http://www.sciencedomain.org/review-history/20517

Original Research Article

Received 2nd July 2017
Accepted 31st July 2017
Published 16th August 2017

ABSTRACT

Oscillatory blood flow in bifurcating arteries with emphasis on the thermal factor is investigated. Blood is treated as Newtonian, viscous, incompressible, homogeneous, magnetically susceptible, chemically reactive but of order one; the arteries are porous, bifurcate axisymmetrically, and have negligible distensibility. The governing non-linear and coupled equations modeled on the Boussinesq assumptions are solved using the perturbation series expansion solutions. The solutions obtained for the temperature and velocity are expressed quantitatively and graphically. The results show that the temperature is increased by the increase in chemical reaction rate, heat exchange parameter, Peclet number, Grashof number and Reynolds number, but decreases with increasing magnetic field parameter (in the range of $0.1 \leq M^2 \leq 1.0$) and bifurcation angle; the velocity increases as the magnetic field parameter (in the range of $0.1 \leq M^2 \leq 1.0$ in the mother channel and $0.1 \leq M^2 \leq 0.5$ in the daughter channel), chemical reaction rate (in the range of $0.1 \leq \delta_1^2 \leq 0.5$), Grashof number (in the range of $0.1 \leq Gr \leq 0.5$), Reynolds number and bifurcation angle. The increase and decrease in the flow variables have strong implications on the arterial blood flow.

**Corresponding author: E-mail: wiaokuyade@gmail.com;*

Keywords: Thermal factor; MHD; mixed convective; blood flow; bifurcating artery.

1. INTRODUCTION

The transport of materials (food nutrients, water, drugs, oxygen and the likes), in particular, round the human body is through the blood. Specifically, in the cardiac cycle of the systemic circulation, the oxygen-rich blood is transported from the heart to other parts of the body. The journey of the oxygen-rich blood starts from the left atrium-ventricle of the heart to the main artery or aorta from which it enters the other arteries connected with such flow like the carotid arteries of the head, subclavian arteries of the fore limbs, gastric and mesenteric arteries of the stomach and intestines, the renal arteries of the kidney, the genital arteries of the gonads, the iliac arteries of the lower limbs and finally to the capillaries and body cells. More so, studies have shown that arteries bifurcate and are sometimes stenosed. At these points, the flow experiences some disturbances due to change in the geometric configurations. The disturbances lead to the emergence of secondary/oscillatory flows. The oscillatory characteristics are marked by the presence of imaginary parts in the solutions of the flow variables.

Furthermore, the rhythmic pumping action of the heart makes the arterial blood flow forced convective. On the other hand, the natural influence of the environmental thermal and concentration gradients accounts for the free convective motion of blood in the human system. For the forced-free convective effects, the arterial blood flow is mixed convective.

There are a lot of literatures on the oscillatory flow in bifurcated, stenosed arteries and other related channels. For example, [1] investigated the radiative heat transfer to blood through a stenosed artery using analytic series solutions, and observed that increase in the height of the constriction increases the heat transfer rate and skin friction; the increase in the radiation absorption parameter increases the velocity, temperature, heat transfer rate and skin friction; the increase in the Hartmann number decreases the flow velocity; [2] studied the effects of heat transfer on the pulsatile blood flow in tubes with slowly varying cross-sections using the perturbation series expansions, and noticed that the amplitude of the pulse, height of constriction and Reynolds number of the flow increase the temperature and heat transfer rates. [3] investigated analytically the oscillatory blood flow in convergent and divergent channels using the method of regular perturbation series solutions, and found that the variations in the pulse amplitude and height of constriction reduce the axial velocity and pressure but increase the radial velocity and wall shear stress. More so, they observed that flow separation occurs in the radial velocity and pressure structures in the convergent and divergent regions respectively, when the height of the constriction is increasingly varied. [4] examined the effects of Reynolds number on the oscillating flow in convergent and divergent channels using the method of perturbation series solutions, and saw that increase in the Reynolds number increases the velocities and wall shear stress. Similarly, they observed that a flow separation occurs in the radial velocity flow structure. [5] investigated the effect of pulse amplitude, radius of constriction and Reynolds number on the blood flow through a multi-stenosed artery under the influence of viscous dissipation and insignificant free convective force. They assumed blood is Newtonian and the artery rigid, and using the stream function and vorticity and perturbation series expansions, and found that an increase in the amplitude decreases the axial pressure and radial velocity; an increase in the height of constriction increases the axial pressure but decreases the radial velocity; an increase in the Reynolds number decreases the radial velocity but has no significant effect on the axial pressure.

The effects of magnetic field on oscillatory arterial blood flow have been investigated. [6] worked on the effects of magnetic field on the flow in a mildly constricted artery, assuming blood is Newtonian, and using the vorticity stream function and Galerkin technique of the finite element method, observed that at increase in the magnetic field intensity flattens the wall shear stress. [7] considered the heat transfer effect on the oscillatory arterial blood flow modeled under the optically fluid assumption using the closed-form solutions, and saw that the height of constriction of the stenosed artery, magnetic field and the heat transfer affect the velocity and temperature distributions; [8] studied the MHD oscillatory flow in a channel filled with porous medium using the closed form solutions method, and observed that increase in magnetic field reduces the wall shear stress while the

radiation parameter increases it. [9] examined the oscillatory blood in multi-stenosed arteries using a vorticity-stream function and finite difference scheme, and noticed that magnetic field increases the heat transfer rate and the thermal boundary layer thickness**.** [10] studied the free convection flow through a vertical porous channel in the presence of an applied magnetic field using the finite difference numerical approach, and noticed that the velocity decreases with the increase in the Darcy and Hartmann numbers. [11] considered the MHD free convective and oscillatory flow through a vertical channel filled with porous medium with non-uniform wall temperatures using the method of asymptotic expansions, and noticed that the fluid velocity, skin-friction coefficient increase as the Grashof number increases; the temperature and velocity and rate of heat transfer of the fluid decrease as porosity and magnetic field, radiation, heat generation/absorption parameters or Prandtl number increases. [12] investigated analytically the effect of heat and mass transfer on the MHD oscillatory flow in an asymmetric wavy channel in the presence of chemical reaction and heat source using the method of regular perturbation, and found that the heat transport of a system is strongly increased in oscillatory flow than in the ordinary condition. [13] considered the radiation and hall current effects on the MHD free convective three -dimensional flow of an incompressible viscous fluid between vertical parallel plates channel filled with a porous medium, and saw among others, that the velocity component for the primary flow increases with the increase in Reynolds number, Darcy parameter, hall parameter, Grashof number, Peclet number and pressure gradient but reduces as the Hartmann number and radiation parameter increase; the velocity component for secondary flow increases with the increase in Darcy number and hall parameter but reduces with the increase in Reynolds number, magnetic field, Gashof number, Peclet number, pressure gradient and radiation parameter.

Furthermore, the roles of geometry with respect to bifurcation angle has been examined. [14] investigated a three-dimensional one-to-two symmetrical flow in which the mother is straight and of circular cross-section, containing a fully developed incident motion, while the diverging daughters are straight and of semi-circular cross-section. Using the method of direct numerical simulation and slender modeling for a variety of Reynolds number and divergent angles, they observed that a flow separation or reversal occurs at the corners of the junction, and the inlet pressure increases as the bifurcation angle increases. [15] considered the flow in a bifurcating river, and found that bifurcation angle, Reynolds number and thermal differentials increase the velocity factor, while the Hartmann number decreases it. [16] investigated analytically the biomechanics of a bifurcating green plant using the perturbation method of solutions, and noticed amidst others, that increase in the bifurcation angle increases the flow velocity and concentration, Nusselt and Sherwood numbers. [17] studied the oscillatory flow in bifurcating green plants using the regular perturbation series solution, and noticed that the velocity increases with the increase in the magnetic field in the range of $0.1 \leq M^2 \leq 1.0$ but drops for $M^2 \geq 5.0$; Reynolds and Peclet numbers increase the concentration and velocity; bifurcation angle decreases the concentration but increases the velocity.

Moreover, the flow of fluids in the arteries has been viewed clinically. For example, [18] investigated the dispersion of drugs through lumen catheters into the arterial system using numerical simulation. They observed that the dispersion is improved by the use of multi-lumen devices; the multi-lumen devices have a reduced hydraulic resistance to blood flow. [19] gave a mass transfer model for predicting the penetration of drugs into the arterial walls by numerical approach, and noticed that the concentration of the drugs at certain depth of the arterial wall depends on the duration of the drug administration, increase with the applied pressure but decreases for lighter viscosities of the advection fluids; [20] studied experimentally the rate of penetration of drugs into the arterial walls using pressured balloon. The study is partly aimed at examining the formation of aneurysms. Also, [21] examined experimentally the roles of waveforms on the flow distribution in cerebral aneurysms, and saw amidst others, that a reduction in the pressure variable gives a universal relationship that characterized the flow; [22] considered the importance of surrounding tissues on the deformation and distensibility of healthy and diseased arteries, and found that the presence of plague reduces the distensibility of the arteries.

Attempting to have an in-depth understanding of flow in physiologic systems, [17] studied the flow of a bio-fluid (the soil mineral salt water) under

oscillatory influence in a bifurcating green plant wherein the inertia force is zero. In this study, we investigate the oscillatory flow behaviour of blood in a bifurcating artery wherein the inertia force is non-zero. Therefore, this work is an extension of [17].

The purpose of this paper is to investigate the oscillatory flow characteristics behaviours of blood in bifurcating arteries under the influence of exposed magnetic field, temperature differentials, Peclet number, Reynolds number, and chemical reaction rate and bifurcation angle.

This paper is arranged in the following order: section 2 is the methodology; section 3 is the results and discussion, while section 4 gives the conclusion.

2. METHODOLOGY

We consider the problem of thermally driven MHD mixed convective oscillatory blood flow in bifurcating arteries. It is formulated under the following assumptions: That arteries are cylindrical, porous, have negligible distensibility, and bifurcate axisymmetrically; Blood is Newtonian, viscous, incompressible, homogeneous, magnetically susceptible, chemically reactive but of order one; the flow velocity is symmetrical in the θ-axis such that its variation about θ-axis is zero, thus for a two-dimensional consideration the velocity components become (u', w') .in the (r', x') coordinates. Therefore, the equations for the continuity, momentum, energy and diffusion respectively, following the Boussinesq approximations are:

$$\frac{1}{r'}\frac{\partial(r'u')}{\partial r'}+\frac{\partial u'}{\partial x'}=0 \tag{1}$$

$$u'\frac{\partial u'}{\partial r'}+w'\frac{\partial u'}{\partial x'}=-\frac{\partial p'}{\partial r'}+\mu\left(\frac{\partial^2 u'}{\partial r'^2}+\frac{1}{r'}\frac{\partial u'}{\partial r'}-\frac{u'}{r'^2}+\frac{\partial^2 u'}{\partial x'^2}\right) \tag{2}$$

$$u'\frac{\partial w'}{\partial r'}+w'\frac{\partial w'}{\partial x'}=-\frac{\partial p'}{\partial x'}+\mu\left(\frac{\partial^2 w'}{\partial r'^2}+\frac{1}{r'}\frac{\partial w'}{\partial r'}+\frac{\partial^2 w'}{\partial x'^2}\right)+\rho' g\beta_t\left(T'-T_\infty'\right)+\rho' g\beta_c\left(C'-C_\infty'\right)$$

$$-\frac{\mu v'}{\kappa}-\frac{\sigma_e B_o^2 w'}{\rho'^2\mu_m} \tag{3}$$

$$\rho C_p\left(u'\frac{\partial T'}{\partial r'}+w'\frac{\partial T'}{\partial x'}\right)=k_o\left(\frac{\partial^2 T'}{\partial r'^2}+\frac{1}{r'}\frac{\partial T'}{\partial r'}+\frac{\partial^2 T'}{\partial x'^2}\right)-Q\left(T'-T_\infty\right) \tag{4}$$

$$u'\frac{\partial C'}{\partial r'}+w'\frac{\partial C'}{\partial x'}=D\left(\frac{\partial^2 C'}{\partial r'^2}+\frac{1}{r'}\frac{\partial C'}{\partial r'}+\frac{\partial^2 C'}{\partial x'^2}\right)+k_r^2\left(C'-C_\infty\right) \tag{5}$$

where p' is the fluid pressure, μ is the fluid viscosity, μ_m is the magnetic permeability of the fluid, g is the gravitational field vector, T' and C' are the fluid temperature and concentration, T_w and C_w are the constant temperature and concentration at the wall, T_∞ and C_∞ are the equilibrium temperature and concentration, B_t and B_c are the volumetric expansion coefficients for temperature and concentration, κ is the permeability of the porous medium, B_o^2 is the applied uniform magnetic field strength due to the salinity of blood, σ_e is the electrical conductivity of blood, k_o is the thermal conductivity of the medium, C_p is the specific heat capacity at constant pressure, Q is the heat absorption/generation coefficient, D is the diffusion coefficient, k_r^2 is the chemical reaction rate.

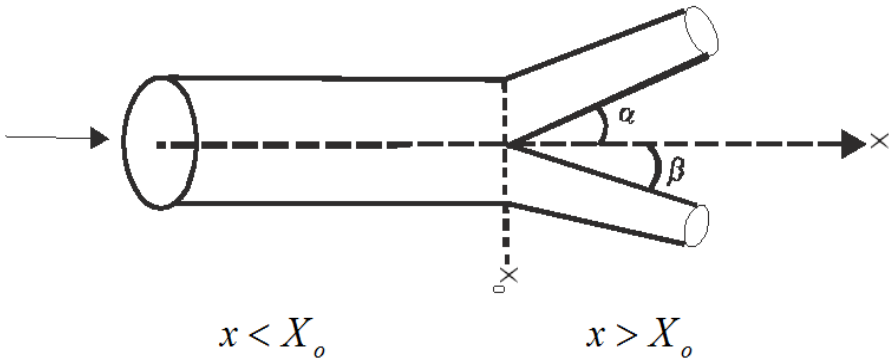

Fig. 1. A physical models of a bifurcating artery (where the angles α and β aresymmetrical)

Fig. 1 shows that the boundary conditions can be separated into two parts: the mother/upstream $x<x_o$ and daughter/downstream $x>x_o$, where x_o is the point of bifurcation assumed the origin. Now for the mother/upstream region we have

$$u'=1,\ w'=1,\ T'=1,\ C'=1 \text{ on } r'=0 \quad (6)$$

$$u'=0,\ w'=0,\ T'=T_w,\ C'=C_w, \text{ on } r'=1 \quad (7)$$

and for the daughter/downstream region

$$u'=0,\ w'=0,\ T'=0,\ C'=0 \text{ on } r'=0 \quad (8)$$

$$u'=0,\ w'=0,\ T'=\gamma_1 T_w,\ C'=\gamma_2 C_w,\ \gamma_1=\gamma_2<1 \text{ on } r'=\alpha x' \quad (9)$$

where α is bifurcation angle, γ_1 and γ_2 are constants.

We introduce the dimensionless variables as:

$$r=\frac{r'}{r_o},\ x=\frac{\Re x'}{l},\ w=\frac{w'r_o}{\upsilon},\ \Theta=\frac{T'-T_\infty}{T_w-T_\infty},\ \Phi=\frac{C'-C_\infty}{C_w-C_\infty},$$

$$p=\frac{(p'-p_\infty)r_o^3}{\rho l\upsilon},\ \mathrm{Re}=\frac{Ul}{\upsilon},\ M^2=\frac{\sigma_e B_o^2}{\rho\mu\mu_m},$$

$$N^2=\frac{Q}{k},\ \chi^2=\frac{r_o}{\kappa},$$

$$\delta_1^2=\frac{k_r^2}{D},\ Sc=\frac{\upsilon}{D},\ \mathrm{Pr}=\frac{\mu C_p}{k},$$

$$Gr=\frac{g\beta_t(T_w-T_\infty)}{\upsilon^2},\ Gc=\frac{g\beta_c(C_w-C_\infty)}{\upsilon^2}$$

where $0<\Re=\frac{r_o}{l}<1$, Θ and Φ are the dimensionless temperature and concentration, respectively; (u,w) are the dimensionless velocities in the (r,x)-axes, $\Re$ is the aspect ratio, υ is the kinematic viscosity, r_o is the characteristic radius of the artery, M^2 is the magnetic field parameter, Re is the Reynolds number, N^2 is the environmental temperature differential parameter, χ^2 is the porosity parameter, δ_1^2 is the chemical reaction parameter, Sc is the Schmidt number, Pr is the Prandtl number, Gr and Gc are the Grashof numbers due to the temperature and concentration difference, respectively; Pe_h and Pe_m are the Peclet number due to heat and mass transfers, respectively; into equations (1) – (9) to have

$$\frac{1}{r}\frac{\partial(ru)}{\partial r}+\frac{\Re\partial w}{\partial x}=0 \quad (10)$$

$$\frac{\partial^2 u}{\partial r^2}+\frac{1}{r}\frac{\partial u}{\partial r}-\frac{u}{r^2}=\frac{\Re\partial p}{\partial x} \quad (11)$$

$$\frac{\partial^2 w}{\partial r^2}+\frac{1}{r}\frac{\partial w}{\partial r}+\Re^2\frac{\partial^2 w}{\partial x^2}-\left(M^2+\chi^2+\Re\frac{\partial w}{\partial x}\right)w=\Re\frac{\partial p}{\partial x}+u\frac{\partial w}{\partial r}-Gr\Theta-Gc\Phi \quad (12)$$

$$\frac{\partial^2 \Theta}{\partial r^2}+\frac{1}{r}\frac{\partial \Theta}{\partial r}+\Re^2\frac{\partial^2 \Theta}{\partial x^2}-N^2\Theta=Pe_h\left(u\frac{\partial \Theta}{\partial x}+\Re w\frac{\partial \Theta}{\partial x}\right) \quad (13)$$

$$\frac{\partial^2 \Phi}{\partial r^2}+\frac{1}{r}\frac{\partial \Phi}{\partial r}+\Re^2\frac{\partial^2 \Phi}{\partial x^2}+\delta_1^2\Phi=Pe_m\left(u\frac{\partial \Phi}{\partial x}+\Re w\frac{\partial \Phi}{\partial x}\right) \quad (14)$$

with the boundary conditions

$$u=1,\ w=1,\ \Theta=1,\ \Phi=1 \ \text{ at } \ r=0 \quad (15)$$

$$u=0,\ w=0,\ \Theta=\Theta_w\ \Phi=\Phi_w \ \text{ at } \ r=1 \quad (16)$$

for the upstream/mother region

$$u=0, w=0,\ \Theta=0,\ \Phi=0 \ \text{ at } \ r=0 \quad (17)$$

$$u=0, w=0, \Theta=\gamma_1\Theta_w, \Phi=\gamma_2\Phi_w,\ \gamma_1<1,\ \gamma_2<1 \ \text{ at } \ r=\Re\alpha x \quad (18)$$

for the downstream/daughter region.

Equation (12) is the crux of this study.

A close look at equations (12)-(14) shows that they are non-linear and coupled. To make them tractable, we assume the flow is fully developed such that $\frac{\partial u}{\partial r}=0$ and equations (10) - (14) drop to:

$$\frac{\partial w}{\partial x}=0 \quad (19)$$

$$\frac{\partial p}{\partial r}=0 \quad (20)$$

$$\frac{\partial^2 w}{\partial r^2}+\frac{1}{r}\frac{\partial w}{\partial r}+\Re^2\frac{\partial^2 w}{\partial x^2}-\left(M^2+\chi^2+\Re\frac{\partial w}{\partial x}\right)w=\Re\frac{\partial p}{\partial x}-Gr\Theta-Gc\Phi \quad (21)$$

$$\frac{\partial^2 \Theta}{\partial r^2}+\frac{1}{r}\frac{\partial \Theta}{\partial r}+\Re^2\frac{\partial^2 \Theta}{\partial x^2}-N^2\Theta=Pe_h\Re w\frac{\partial \Theta}{\partial x} \quad (22)$$

$$\frac{\partial^2 \Phi}{\partial r^2}+\frac{1}{r}\frac{\partial \Phi}{\partial r}+\Re^2\frac{\partial^2 \Phi}{\partial x^2}+\delta_1^2\Phi=Pe_m\Re w\frac{\partial \Phi}{\partial x} \quad (23)$$

with the boundary conditions

$$w=1,\ \Theta=1,\ \Phi=1 \quad \text{at } \ r=0 \quad (24)$$

$$w=0\ ,\Theta=\Theta_w\ ,\ \Phi=\Phi_w \ \text{ at } \ r=1 \quad (25)$$

for the upstream region

$$w=0,\ \Theta=0,\ \Phi=0 \quad \text{at } \ r=0 \quad (26)$$

$$w=0,\ \Theta=\gamma_1\Theta_w,\ \Phi=\gamma_2\Phi_w,\ \gamma_1<1,\ \gamma_2<1 \ \text{ at } \ r=\Re\alpha x \quad (27)$$

for the downstream region

For further simplification and tractability of equations (21)-(27), we seek for the perturbation series solution in terms of the Reynolds number and of the form:

$$h(r,x)=f_o(r,x))+\xi h_1(r,x)+\xi^2 f_2(r,x)+... \quad (28)$$

where $\xi = \frac{1}{\mathrm{Re}} < 1$ the perturbing parameter, is small. The choice of this parameter comes from the fact that in the upstream channel the flow is laminar and Poiseuille such that the Reynolds number is usually moderate. But almost at the point of bifurcation, the inertial force and hence the Reynolds number rises due to a change in the geometrical configuration. This being the case, its reciprocal will be small enough. More so, we assume the velocity, temperature and concentration variables h_n can be expressed as: $h_0(r,x) = h_{00}(r) - \gamma x$ and $h_1(r,x) = h_{10}(r) - \gamma x$ and the pressure as $p(x) = \aleph x - \gamma x^2$, where $\aleph x$ is the upstream pressure, and γx^2 is the downstream pressure (see [23]). Substituting these into equations (21)-(27) gives

$$\frac{\partial^2 w_{00}}{\partial r^2} + \frac{1}{r}\frac{\partial w_{00}}{\partial r} - \left(M^2 + \chi^2 - \Re\gamma\right)w_{00} = \Re\aleph - Gr\Theta_{00} - Gc\Phi_{00} \tag{29}$$

$$\frac{\partial^2 \Theta_{00}}{\partial r^2} + \frac{1}{r}\frac{\partial \Theta_{00}}{\partial r} + N^2\Theta_{00} = -\gamma\Re Pe_h w_o \tag{30}$$

$$\frac{\partial^2 \Phi_{00}}{\partial r^2} + \frac{1}{r}\frac{\partial \Phi_{00}}{\partial r} + \delta_1^{\,2}\Phi_{00} = -\gamma\Re Pe_m w_o \tag{31}$$

$$\frac{\partial^2 w_{10}}{\partial r^2} + \frac{1}{r}\frac{\partial w_{10}}{\partial r} - \left(M^2 + \chi^2 - \Re\gamma\right)w_{10} = \Re\aleph_1 x - Gr\Theta_{10} - Gc\Phi_{10} \tag{32}$$

$$\frac{\partial^2 \Theta_{10}}{\partial r^2} + \frac{1}{r}\frac{\partial \Theta_{10}}{\partial r} - N^2\Theta_{10} = Pe_h\Re\gamma\left(w_{00} + w_{10}\right) \tag{33}$$

$$\frac{\partial^2 \Phi_{10}}{\partial r^2} + \frac{1}{r}\frac{\partial \Phi_{10}}{\partial r} + \delta_1^2\Phi_{10} = Pe_h\Re\gamma\left(w_{00} + w_{10}\right) \tag{34}$$

Where $\aleph_1 = 2\gamma$

Now, for the mother/upstream channel, we shall remove w_o from equations (30) and (31) by taking the

$$\left(\frac{\partial^2}{\partial r^2} + \frac{1}{r}\frac{\partial}{\partial r} - M_1^2\right)$$ (where $M_1^2 = M^2 + \chi^2 - \Re\gamma$)

of both equations to get

$$\left[\left(D_r - M_1^2\right)\left(D_r + N^2\right) - \gamma R\varepsilon\right]\Theta_{oo} = \gamma R\varepsilon\Phi_{oo} - \gamma\Re\varepsilon Pe_h\aleph \tag{35}$$

and

$$-\gamma\Re\varepsilon Pe_h\aleph + \gamma R\varepsilon\Theta_{oo} = \left[\left(D_r - M_1^2\right)\left(D_r + \delta_1^2\right) - \gamma R\varepsilon\right]\Phi_{oo} \tag{36}$$

where $D_r = \left(\frac{\partial^2}{\partial r^2} + \frac{1}{r}\frac{\partial}{\partial r}\right)$ and $\varepsilon = Pe_h Gr = Pe_m Gc, Gr = Gc$

Moreover, we shall remove Φ_{oo} from equations (35) and (36) by multiplying through equation (35) by $\gamma R\varepsilon$ and taking

$$\left[\left(D_r - M_1^2\right)\left(D_r + N^2\right) - \gamma R\varepsilon\right]$$

of equation (36) so that on adding the evolving equations, we have

$$\left[\left(D_r - M_1^2\right)\left(D_r + N^2\right) - \gamma R\varepsilon\right]\left[\left(D_r - M_1^2\right)\left(D_r + \delta_1^2\right) - \gamma R\varepsilon\right]\Theta_{oo} = -\gamma R\varepsilon Pe_h \aleph \tag{37}$$

which expands to give

$$\begin{aligned}&\left[D_r^4 + \left(2N^2 + \delta_1^2 - M_1^2\right)D_r^3 + \left(-M_1^2 + 2N^2M_1^2 + 2M_1^2 - N^2\delta_1^2 - M_1^4 - 2\gamma R\varepsilon\right)D_r^2 + \right.\\ &\left.\left(-M_1^4\delta_1^2 - \gamma\Re\varepsilon\left(2N^2 - M^2 - \delta_1^2 + M_1^2N^4\right)\right)D_r + \left(-M_1^2\delta_1^2\gamma\Re\varepsilon + \gamma^2\Re^2\varepsilon^2\right)\right]\Theta_{oo}\\ &= -\gamma R\varepsilon Pe_h\aleph\end{aligned} \tag{38}$$

Equation (38) is a fourth order characteristic equation. We shall break it into two solvable parts: the even and odd powers terms. Thus:

$$\begin{aligned}&\left[D_r^4 + \left(-M_1^2 + 2N^2M_1^2 + 2M_1^2 - N^2\delta_1^2 - M_1^4 - 2\gamma R\varepsilon\right)D_r^2 + \right.\\ &\left.\left(-M_1^2\delta_1^2\gamma\Re\varepsilon + \gamma^2\Re^2\varepsilon^2\right)\right]\Theta_{oo} = -\gamma R\varepsilon Pe_h\aleph\end{aligned} \tag{39}$$

for the even power terms

$$D_r\left[\left(2N^2 + \delta_1^2 - M_1^2\right)D_r^2 + \left(-M_1^4\delta_1^2 - \gamma\Re\varepsilon\left(2N^2 - M^2 - \delta_1^2 + M_1^2N^4\right)\right)\right]\Theta_{oo} = 0 \tag{40}$$

and for the odd powers terms.

Now, since our problem here is of fourth order, the solution of equation (39) which is

$$\Theta_{oo}(r) = d_1 I_o\left(\zeta_8^{1/2} r\right) + \frac{I_o\left(\zeta_8^{1/2} r\right)}{2}\zeta_8^{1/2} c_1 \frac{rI_1\left(\zeta_6^{1/2} r\right)}{\zeta_6^{1/2}} \tag{41}$$

can be used to approximate the solution of equation (38).

Furthermore, we remove Θ_{oo} from equation (35) and equation (36) by taking

$$\left[\left(D_r - M_1^2\right)\left(D_r + \delta_1^2\right) - \gamma R\varepsilon\right]$$

of equation (35) and multiplying through equation (36) by $\gamma R\varepsilon$ so that on subtracting the first from the second, we have

$$\left[\left(D_r - M_1^2\right)\left(D_r + N^2\right) - \gamma R\varepsilon\right]\left[\left(D_r - M_1^2\right)\left(D_r + \delta_1^2\right) - \gamma R\varepsilon\right]\Phi_{oo} = -\gamma R\varepsilon Pe_h\aleph \tag{42}$$

Comparing equation (37) with equation (42), reveals that they are the similar. So, $\Theta_{oo} = \Phi_{oo}$.

More so, putting Φ_{oo} and Θ_{oo} in equation (29) and solving gives

$$w_{oo}(r) = v_1 I_o(M_1 r) - M_1 r I_o(M_1 r)\left[-\frac{\Re\aleph r}{2} + Grd_1 \frac{I_1(\zeta_8^{1/2} r)}{\zeta_6^{1/2}} + \right.$$
$$\left. -\frac{r^5}{20} - \frac{\zeta_6 r^7}{114} + M_1^2\left(\frac{r^4}{16} + \frac{\zeta_6 r^6}{192}\right)\right] + \left(-\frac{M_1 r}{2} + \frac{M_1^2 r^3}{4}\right)\left[\frac{\Re\aleph I_1(M_1 r)}{M_1} - 2Grd_1\left(\frac{I_1(\zeta_8^{1/2} r)}{\zeta_8^{1/2}}\right.\right.$$
$$\left.\left. -\frac{M_1^2 r^3}{6} - \frac{M_1^2 \zeta_8 r^5}{40}\right) + \frac{r^3}{6} + \frac{\zeta_6 r^5}{80} + M_1^2\left(\frac{r^4}{16} + \frac{\zeta_6 r^6}{192}\right)\right] \quad (43)$$

For the daughter/downstream problem, we solve equations (32)-(34). We shall remove w_{oo} and w_{10} from equation (33) and (34) by taking

$$\left(\frac{\partial^2}{\partial r^2} + \frac{1}{r}\frac{\partial}{\partial r} - M_1^2\right)$$

of both sides of the equations, and substituting the solutions of Θ_{oo} and Φ_{oo} [see equation (41)] into the resulting equations gives

$$\left[\left(D_r - M_1^2\right)\left(D_r + N^2\right) - \gamma R\varepsilon\right]\Theta_{10} = \gamma R\varepsilon\Phi_{10} - \gamma R^2 Pe_m\left(\aleph + \aleph_1 x\right) + 2\gamma R\varepsilon d_1 I_o\left(\zeta_8^{1/2} r\right) + \ldots \quad (44)$$

and

$$\left[\left(Dr - M_1^2\right)\left(Dr + \delta_1^2\right) - \gamma R\varepsilon\right]\Phi_{10} = \gamma R\varepsilon\Theta_{10} - \gamma R^2 Pe_m\left(\aleph + \aleph_1 x\right) + 2\gamma R\varepsilon d_1 I_o\left(\zeta_8^{1/2} r\right) + \ldots \quad (45)$$

Also, removing Φ_{10} from equation (44) and (45) by multiplying equation (43) by $\gamma R\varepsilon$ and taking

$$\left[\left(D_r - M_1^2\right)\left(D_r + N^2\right) - \gamma R\varepsilon\right]$$

of equation (45),and subtracting the first result from the second gives

$$\left[\left(D_r - M_1^2\right)\left(D_r - N^2\right) - \gamma\Re\varepsilon\right]\left[\left(D_r - M_1^2\right)\left(D_r - \delta_1^2\right) - \gamma\Re\varepsilon\right]\Theta_{10} - \gamma^2\Re^2\varepsilon^2\Theta_{10}$$
$$= -\gamma^2\Re^3\varepsilon Pe_h\left(N + N_1 x\right) + 2d_1\gamma^2\Re^2\varepsilon^2 I_o\left(\zeta_8^{1/2} r\right) \quad (46)$$

which expands to give

$$\left\{\begin{array}{l} D_r^4 + \left[\left(\delta_1^2 - M_1^2\right)\left(N^2 - M_1^2\right)D_r^3\right] + \left[-M_1^2\delta_1^2 + \left(N^2 - M_1^2\right)\left(\delta_1^2 - M_1^2\right) - M_1^2 N^2\right]D_r^2 \\ \left[-M_1^2\delta_1^2\left(N^2 - M_1^2\right) - \gamma\Re\varepsilon\left(N^2 - M_1^2\right) - M_1^2 N^2\left(\delta_1^2 - M_1^2\right) - \gamma\Re\varepsilon\left(\delta_1^2 - M_1^2\right)\right]D_r + \\ \gamma\Re\varepsilon\left[M_1^2 N^2\delta_1^2 + M_1^2 N^2 + M_1^2\delta_1^2\right] \end{array}\right\}\Theta_{10}$$
$$= \gamma^2\Re^3\varepsilon Pe_h\left(N + N_1 x\right) + D_1\gamma^2\Re^2\varepsilon^2 I_o\left(\zeta_8^{1/2} r\right) \quad (47)$$

To ease solving, we separate equation (47) into two: the even and odd power terms to get

$$\left[D_r^4+\left[-M_1^2\delta_1^2+\left(N^2-M_1^2\right)\left(\delta_1^2-M_1^2\right)-M_1^2N^2\right]D_r^2+\gamma\Re\varepsilon\left[M_1^2N^2\delta_1^2+M_1^2N^2+M_1^2\delta_1^2\right]\right]\Theta_{10}$$
$$=\gamma^2\Re^3\varepsilon Pe_h\left(N+N_1x\right)+D_1\gamma^2\Re^2\varepsilon^2I_o\left(\zeta_8^{1/2}r\right) \quad (48)$$

for the even power terms, and

$$D_r\left[\left[\left(\delta_1^2-M_1^2\right)\left(N^2-M_1^2\right)\right]D_r^2+\left[-M_1^2\delta_1^2\left(N^2-M_1^2\right)-\gamma\Re\varepsilon\left(N^2-M_1^2\right)\right.\right.$$
$$\left.\left.-M_1^2N^2\left(\delta_1^2-M_1^2\right)-\gamma\Re\varepsilon\left(\delta_1^2-M_1^2\right)\right]\right]\Theta_{10}=0 \quad (49)$$

for the odd terms

Solving equation (48), we have

$$\Theta_{10}=k_1\frac{I_o\left(\zeta_{16}^{1/2}r\right)}{2}+I_o\left(\zeta_{16}^{1/2}r\right)\zeta_{16}^{1/2}g_1r\frac{I_o\left(\zeta_{14}^{1/2}r\right)}{\zeta_{14}^{1/2}} \quad (50)$$

and this can be used to approximate the solution of equation (47), being order four.

Similarly, removing Θ_{10} from equation (44) and (45) by multiplying equation (44) by $\gamma R\varepsilon$ and taking $\left[\left(D_r-M_1^2\right)\left(D_r+N^2\right)-\gamma R\varepsilon\right]$

of equation (45), and subtracting the first result from the second gives

$$\left[\left(D_r-M_1^2\right)\left(D_r-N^2\right)-\gamma\Re\varepsilon\right]\left[\left(D_r-M_1^2\right)\left(D_r-\delta_1^2\right)-\gamma\Re\varepsilon\right]\Phi_{10}-\gamma^2\Re^2\varepsilon^2\Phi_{10}$$
$$=-\gamma^2\Re^3\varepsilon Pe_h\left(N+N_1x\right)+2D_1\gamma^2\Re^2\varepsilon^2I_o\left(\zeta_6^{1/2}r\right) \quad (51)$$

Comparing equation (46) with equation (51), reveals that they are the similar. So, $\Theta_{10}=\Phi_{10}$.

Substituting Θ_{10} and Φ_{10} in equation (32) and solving, we have

$$w_1(r)=v_1I_o(M_1r)-I_o(M_1r)\left\{-\frac{\Re\aleph_1xr}{2}+Gc\left[\frac{k_1I_1(\zeta_{16}^{1/2}r)}{\zeta_{16}^{1/2}}+\zeta_{16}^{1/2}g_1\left(\frac{rI_1(\zeta_{16}^{1/2}r)}{\zeta_{16}^{1/2}}+\frac{\zeta_{14}r^4}{64}\right.\right.\right.$$
$$\left.\left.\left.+\frac{\zeta_{14}\zeta_{16}r^6}{384}\right)\right]+\frac{M_1^2}{4}\left[\frac{\Re\aleph_1r^3}{3}-2Gc\left[k_1\left(\frac{r^3}{3}+\frac{\zeta_{16}r^5}{20}\right)+\zeta_{16}^{1/2}g_1\left(\frac{rI_1(\zeta_{16}^{1/2}r)}{2\zeta_{16}^{1/2}}+\right.\right.\right.$$
$$\left.\left.\left.\left.\left.\frac{\zeta_{14}r^4}{64}+\frac{\zeta_{14}\zeta_{16}r^6}{384}\right)\right]\right]\right\}+\left(-\frac{M_1r}{3}+\frac{M_1^3r^3}{4}\right)\left\{-\frac{\Re\aleph_1xI_1(M_1r)}{M_1}\right.$$
$$+2Gc\left[k_1\left(\frac{I_1(M_1r)}{M_1}+\frac{\zeta_{16}r^4}{16}+\frac{M_1^2\zeta_{16}r^5}{80}\right)+\zeta_{16}^{1/2}g_1\left(\frac{rI_1(M_1r)}{2M_1}+\frac{\zeta_{14}r^4}{64}+\frac{\zeta_{14}M_1r^6}{384}\right)+\right.$$
$$\left.\left.\frac{\zeta_{16}r^4}{32}+\frac{\zeta_{16}M_1^2r^6}{192}+\frac{\zeta_{14}\zeta_{16}r^6}{384}+\frac{\zeta_{14}\zeta_{16}M_1^2r^8}{2048}\right]\right\} \quad (52)$$

3. RESULTS AND DISCUSSION

In section 2, the problem of oscillatory blood flow with emphasis on the thermal factor is formulated. The effects of some choice parameters such as M^2, δ_1^2, N^2, Gr/Gc, Pe, Re and α are investigated. The computation is carried out using Maple 18for constant realistic values of Pr =0.71, γ_1 = 0.6, γ_2 =0.6, γ =0.7, Φ_w = 2.0, Θ_w =2.0, $\Re = 0.8$ and varying values of δ_1^2 =0.1, 0.3, 0.5, 1.0, 5.0; M^2 = 0.1, 0.3, 0.5, 1.0, 5.0; N^2=0.1, 0.3, 0.5, 1.0, 5.0; Gr/Gc=0.1, 0.3, 0.5, 1.0, 5.0; Pe=0.1, 0.3, 0.5, 1.0, 5.0; Re=100, 500, 1000, 2000, 3000; α=5, 10, 15, 20, 25. The results are shown below. Figs. 2-4 and Tables 1-11 show that the temperature distribution is increased by the increase in chemical reaction rate, heat exchange parameter, Peclet number, Grashof numbers, and Reynolds number but it is decreased by the increase in the magnetic field parameter (in the range $0.1 \le M^2 \le 1.0$), and bifurcation angle; the velocity distribution is increased by the increase in magnetic field parameter (in the range $0.1 \le M^2 \le 0.5$), chemical reaction rate, Grashof numbers (in the range $0.1 \le Gr \le 0.5$), Reynolds number and bifurcation angle.

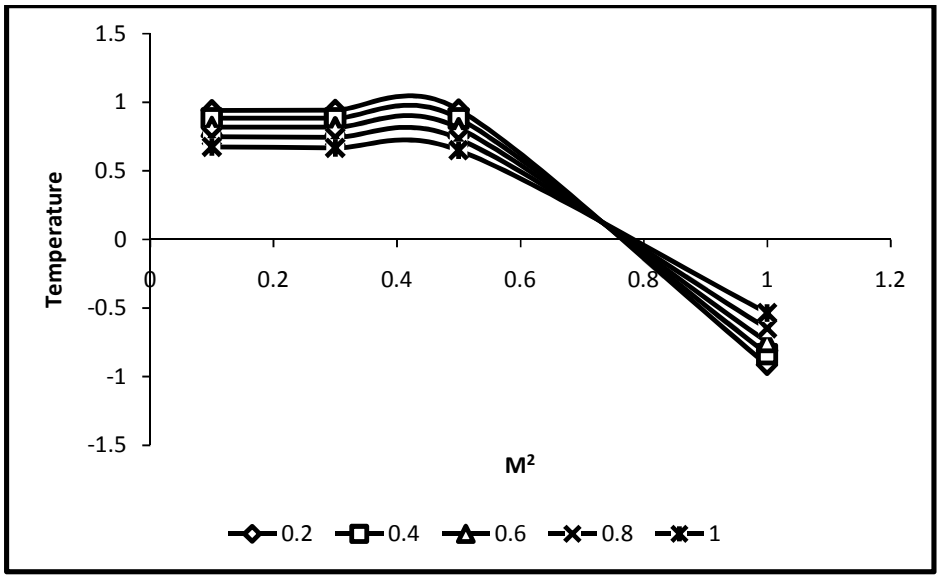

Fig. 2. Temperature-magnetic field parameter profiles in the mother channel

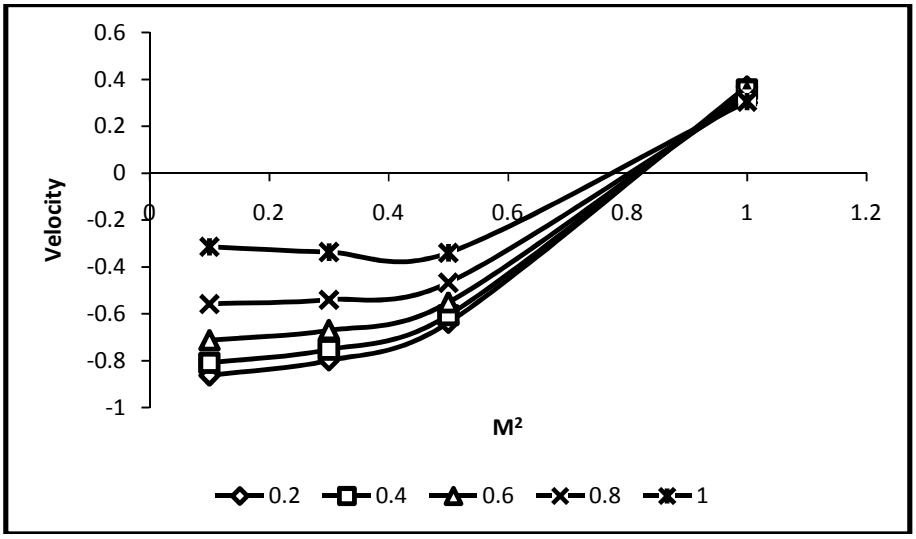

Fig. 3. Velocity-magnetic field parameter profiles in the mother channel

Fig. 2 shows that the temperature decreases with the increase in the magnetic field strength. Also, the distribution have a flow separation structure at r=0.7. The presence of flow separation may be due to some adverse conditions in the flow field. More so, Fig.3 and Table 1 show that the velocity distribution increases with the increase in the magnetic field strength in certain ranges, and after which it drops. In the mother channel, It increases within $0.1 \leq M^2 \leq 1.0$ while in the daughter, it increases within $0.1 \leq M^2 \leq 0.5$.The fluctuation in the velocity may be due to the oscillatory effect.

Table 1. Velocity-magnetic field parameter in the daughter channel

r	M^2=0.1	M^2=0.3	M^2=0.5	M^2=1.0	M^2=5.0
0.2	-2.75109 I	2.84872 I	25.1280 I	-22.2304 I	-297.945 I
0.4	-2.75009 I	2.84772 I	25.1180 I	-22.2204 I	-297.925 I
0.6	-2.74935 I	2.85559 I	25.3042 I	-22.8749 I	-476.682 I
0.8	-2.74896 I	2.86901 I	25.6168 I	-23.9692 I	-774.619 I
1.0	-2.76340 I	2.92424 I	26.6820 I	-27.5023	-1728.14 I

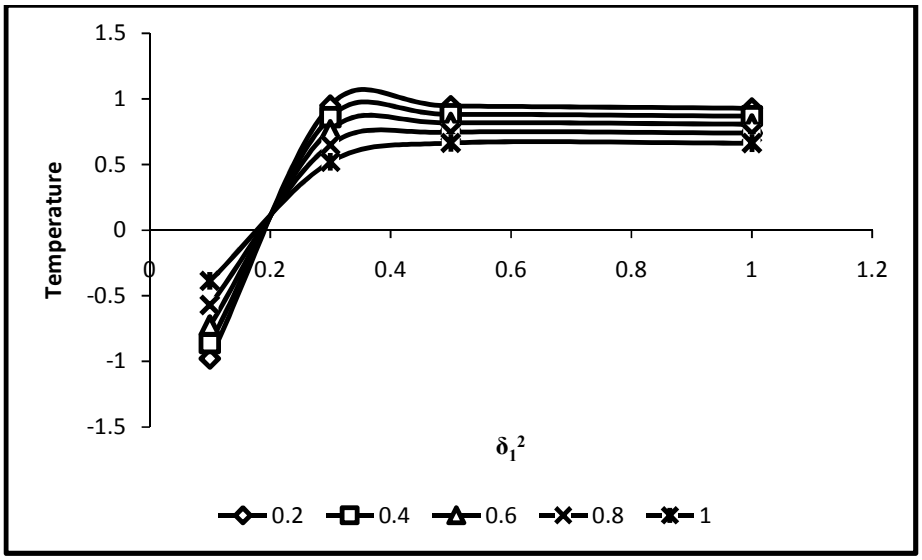

Fig. 4. Temperature-chemical reaction rate in the mother channel

Table 2. Temperature-chemical reaction rate in the daughter channel

R	δ_1^2=0.1	δ_1^2=0.3	δ_1^2=0.5	δ_1^2=1.0	δ_1^2=5.0
0.2	0.129135 I	0.146072 I	0.172567 I	0.249870 I	0.785695 I
0.4	0.128107 I	0.144936 I	0.171287 I	0.248343 I	0.789444 I
0.6	0.126184 I	0.142783 I	0.168802 I	0.245093 I	0.788970 I
0.8	0.123045 I	0.139217 I	0.164578 I	0.239043 I	0.774393 I
1.0	0.118234 I	0.133673 I	0.157852 I	0.228660 I	0.730024 I

Table 3. Velocity-chemical reaction rate in the mother channel

r	δ_1^2=0.1	δ_1^2=0.3	δ_1^2=0.5	δ_1^2=1.0
0.2	-0.729313 I	-0.703236 I	-0.693916 I	-0.703066 I
0.4	-0.694784 I	-0.668733 I	-0.657240 I	-0.665003 I
0.6	-0.633679 I	-0.608046 I	-0.593062 I	-0.598432 I
0.8	-0.537427 I	-0.513930 I	-0.493668 I	-0.495527 I
1.0	-0.387330 I	-0.366534 I	-0.342068 I	-0.339182 I

Fig. 3 and Table 2 show that the temperature increases as the rate of chemical reaction increases. Similarly, the figure shows the existence of flow separation in the temperature distribution at r=0.2. Furthermore, Table 3 depicts that the velocity distribution increases with the increase in the rate of chemical reaction in the range of $0.1 \leq \delta_1^2 \leq 0.5$ but drops for $\delta_1^2 = 1.0$. The fluctuation in the velocity structure may be due to the oscillatory effect. Chemical reaction leads to the depletion of the chemicals in the fluid system. It may be heat absorbing or generating. Specifically, the increase in the fluid temperature may imply that the chemical reaction is heat-generating.

Table 4 shows that the fluid temperature distribution increases with the increase in the heat exchange parameter. A positive heat gradient exists between man and his environment when the radiation from the sun increases or when he is drawn near to a source of heat. In such situations heat is usually absorbed from the external source into the body; thus increasing the body fluid temperature.

Table 5 shows that the fluid temperature increases as the Grashof number increases. More so, Table 6 depicts that the velocity distribution increases with the increase in the Grashof number within the range of $0.1 \leq Gr \leq 0.5$ but drops for $Gr \geq 1.0$. The fluctuation in the velocity field may be due to the oscillatory factor. As said above, a positive thermal gradient exists between the man and his environment when the external heat level is higher than the body equilibrium temperature. The temperature gradient sparks up the free convective current (Grashof number) which reduces the viscosity of the fluid and energizes the fluid particles to higher motion.

Table 4. Temperature-Heat exchange parameter in the daughter channel

r	N^2=0.1	N^2=0.3	N^2=0.5	N^2=1.0	N^2=5.0
0.2	0.128107 I	0.144936 I	0.171287 I	0.248343 I	0.789444 I
0.4	0.128109 I	0.144939 I	0.171289 I	0.248345 I	0.789446 I
0.6	0.126184 I	0.142783 I	0.168802 I	0.245092 I	0.788970 I
0.8	0.123045 I	0.139217 I	0.164577 I	0.239043 I	0.774040 I
1.0	0.118235 I	0.133673 I	0.157852 I	0.228659 I	0.730024 I

Table 5. Temperature-Grashof number in the daughter channel

r	Gr=0.1	Gr=0.3	Gcr=0.5	Gr=1.0	Gcr=5.0
0.2	0.219180 I	0.308713 I	0.378750 I	0.539227 I	5.20106 I
0.4	0.217406 I	0.306034 I	0.375359 I	0.534237 I	5.15795 I
0.6	0.214037 I	0.301007 I	0.369032 I	0.524980 I	5.07743 I
0.8	0.208440 I	0.292771 I	0.358727 I	0.510007 I	4.94596 I
1.0	0.199705 I	0.280079 I	0.342932 I	0.487188 I	4.74349 I

Table 6. Velocity- Grashof number in the daughter channel

r	Gr=0.1	Gr=0.3	Gc=0.5	Gr=1.0	Gc=5.0
0.2	0.299401 I	1.81187 I	6.20444 I	-4.29062 I	-25.8483 I
0.4	0.301328 I	1.82321 I	6.24211 I	-4.27821 I	-25.9327 I
0.6	0.304518 I	1.84209 I	6.30529 I	-4.26882 I	-26.0934 I
0.8	0.309041 I	1.86914 I	6.39664 I	-4.27720 I	-26.3578 I
1.0	0.315175 I	1.90636 I	6.52417 I	-4.32723 I	-26.7747 I

Table 7. Temperature-Peclet number in the daughter channel

r	Pe=0.1	Pe=0.3	Pe=0.5	Pe=1.0	Pe=5.0
0.2	0.184592I	0.245728I	0.289355I	0.378750I	1.13127 I
0.4	0.183161I	0.243688I	0.286873I	0.375359I	1.12085 I
0.6	0.18419I	0.239831I	0.282205I	0.369032I	1.10156 I
0.8	0.175823I	0.233455I	0.274543I	0.358727I	1.07042 I
1	0.168596I	0.223552I	0.262709I	0.342932I	1.02303 I

Table 7 shows that the temperature increases as the Peclet number increases. Peclet number is the ratio of the product the channel length and fluid local velocity to the thermal/concentration diffusivity. Assuming the thermal diffusivity is constant, the increase in the Peclet number depicts that the velocity is increasing. Furthermore, the increase in the velocity favours the temperature, and vice versa.

Table 8 shows that the fluid temperature increases with the increase in the Reynolds number. More so, Table 9 shows that the velocity increases with the increase in the flow Reynolds number. In the mother tube the flow is laminar and Poiseuille such that its Reynolds number is moderate. But almost at the point of bifurcation the inertial force rises due to the change in the geometrical configuration, and so are the Reynolds number and momentum. These increases favour the velocity, which in turn increases the temperature. These results agree with [4] and [13].

Table 10 shows that the temperature decreases with the increase in the bifurcation angle. Additionally, Table 11 depicts that the flow velocity increases as the bifurcation angle increases. It is seen from Fig.1 that the increase in the bifurcation angle tends to narrow down the daughter channels. In effects, this has the tendency of increasing the inlet pressure, which invariably increases the velocity and temperature. Therefore, the decrease in the temperature may be due to oscillatory effect. These results align with [14,16,17].

Table 8. Temperature-reynolds number in the daughter channel

r	Re=100	Re =500	Re =1000	Re =2000	Re =3000
0.2	0.027507I	0.041260I	0.082520I	0.165039I	0.825196I
0.4	0.027300I	0.040949I	0.081899I	0.163797I	0.818985I
0.6	0.026900I	0.040351I	0.080701I	0.161403I	0.807014I
0.8	0.026227I	0.039341I	0.078682I	0.157364I	0.786820I
1	0.025163I	0.037744I	0.075489I	0.150978I	0.754889I

Table 9. Velocity-reynolds number in the daughter channel

r	Re=100	Re=500	Re=1000	Re=2000	Re=3000
0.2	1.03407 I	1.55111 I	3.10221 I	6.20442 I	31.02210 I
0.4	1.04035 I	1.56028 I	3.12106 I	6.24211 I	31.21055 I
0.6	1.05088 I	1.57632 I	3.15265 I	6.30529 I	31.52646 I
0.8	1.06611 I	1.59916 I	3.19832 I	6.39664 I	31.98132 I
1	1.08762I	1.63104 I	3.26209 I	6.52417 I	32.62087 I

Table 10. Temperature-bifurcation angle in the daughter channel

r	α=5	α =10	α =15	α =20
0.2	0.520105 I	-36.6510 I	-265.550 I	-777.910 I
0.4	0.518794 I	-36.2090 I	-258.180 I	-748.390 I
0.6	0.515791 I	-36.1710 I	-257.120 I	-746.330 I
0.8	0.494596 I	-34.2510 I	-228.450 I	-630.070 I
1	0.474349 I	-32.7610 I	-206.090 I	-541.250 I

Table 11. Velocity-bifurcation angle in the daughter channel

r	α=5	α =10	α =15	α =20
0.2	0.620442I	567.477I	1194.89I	6802.17I
0.4	0.624211I	571.020I	1202.12I	6843.06I
0.6	0.630529I	576.888I	1214.16I	6911.17I
0.8	0.639664I	585.033I	1230.97I	7006.44I
1	0.65242I	595.420I	1252.54I	7128.83I

The increase or decrease in the flow variables has characteristic implications on the transport of blood in bifurcating arteries. Specifically, the increase in the temperature reduces the fluid viscosity and makes the arterial walls more permeable. Subsequently, these increase the rate of the blood transport to other parts of the body.

4. CONCLUSION

The oscillatory flow of blood in bifurcating arteries with emphasis on the thermal factor is considered. The effects of increasing magnetic field parameter, chemical reaction rate, heat exchange parameter, Peclet number, Grashof number, Reynolds number and bifurcation angle are investigated. The results show that the temperature is increased by the increase in chemical reaction rate, heat exchange parameter, Peclet number, Grashof number and Reynolds number but decreases with increasing magnetic field parameter (in the range of $0.1 \leq M^2 \leq 1.0$) and bifurcation angle; the velocity increases as the magnetic field parameter (in the range of $0.1 \leq M^2 \leq 1.0$ in the mother channel and $0.1 \leq M^2 \leq 0.5$ in the daughter channel), chemical reaction rate (in the range of $0.1 \leq \delta_1^2 \leq 0.5$), Grashof number (in the range of $0.1 \leq Gr \leq 0.5$), Reynolds number and bifurcation angle. The increase and decrease in the flow variables have strong implications on the bifurcating arterial blood flow.

COMPETING INTERESTS

Authors have declared that no competing interests exist.

REFERENCES

1. Prakash J, Makinde OD. Radiative heat transfer to blood low through a stenotic artery in the presence o magnetic field. Latin America Applied Research. 2011; 41(3):273-277.
2. Okuyade WIA, Mbeledogu IU, Abbey TM. Heat transfer effects on an oscillatory blood flow in tubes with slowly varying cross-sections. Asian Journal of Applied Sciences. 2015;3(6):770-782.
3. Okuyade WIA, Abbey TM. Oscillatory blood flow in convergent and divergent channels, Part 1-Effects of pulse amplitude and local constriction height. British Journal of Mathematics and Computer Science (Science Domain International). 2016a;14(6):1-17. DOI: 10.9734/BJMCS/2016/23221.
4. Okuyade WIA, Abbey TM. Oscillatory blood flow in convergent and divergent channels, Part 2-. Effects of Reynolds number. British Journal of Mathematics and Computer Science (Science Domain International). 2016b;15(1):1-14. DOI: 10.9734/BJMCS/2016/23222
5. Okuyade WIA. Peristaltic transport with viscous dissipation effect in a multi-stenosed artery. Asian Research Journal of Mathematics. 2017;5(2):1-18. DOI: 10.9734/ARJOM/2017/31459
6. Amos E, Ogulu A. Indian Journal of Pure and Applied Mathematics. 2003;34(9): 1315.
7. Ogulu A, Abbey TM. Simulation of heat transfer on an oscillatory blood flow in an indented porous artery. International Communications in Heat and Mass Transfer. 2005;32:983–989.
8. Makinde OD, Mhone PY. Heat transfer to MHD oscillatory flow in a channel filled with porous medium. Romania Journal of Physics. 2005;50(9-10):931-938.
9. Bourhan Tashtoush, Ahmad Magableh. Magnetic field effect on heat transfer and fluid flow characteristics of blood flow in multi-stenosis arteries. Journal of Heat Mass Transfer. 2008;44:297–304. DOI 10.1007/s00231-007-0251-x
10. Venkateswalu S, Suryanarayama Rao KV, Rambupal Reddy B. Finite difference analysis on convective heat transfer flow through porous medium in a vertical channel with magnetic field. Indian Journal of Applied Mathematics and Mechanics. 2011;7(7):74–94.
11. Sharma PR, Kalpna Sharma, Tripti Mehta. Radiative and free convective effects on MHD flow through a porous medium with periodic wall temperature and heat generation or absorption. International Journal of Mathematical Archive. 2014; 5(9):119-128.
12. Satya PV Narayana, Venkateswarlu B, Devika B. Chemical reaction and heat source effects on MHD oscillatory flow in an irregular channel. Ain Shams Engineering Journal; 2015.
13. Krishna MV, Basha SC. MHD free convection three dimensional flow through a porous medium between two vertical plates. International Organization of

Scientific Research Journal of Mathematics. 2016;88-105.
DOI: 10.9790/5728-121288105

14. Tadjar M, Smith FT. Direct simulation and modeling of basic 3-dimensional bifurcating tube flow. Journal of Fluid Mechanics. 2004;519:1-32.
15. Okuyade WIA, Abbey TM, Steady MHD fluid flow in a bifurcating rectangular porous channel. Advances in Research (Sciencedomain International). 2016c; 8(3):1-17.
DOI: 10.9734/AIR2016.26399
16. Okuyade WIA, Abbey TM. Biomechanics of a bifurcating green plant, part 1. Asian Journal of Physical and Chemical Sciences (ScienceDomain International). 2016d; 1(2):1-22.
DOI: 10.9734/AJOPS/2016/31458
17. Okuyade WIA, Abbey TM. Steady oscillatory flow in a bifurcating green plant, Asian Research Journal of Mathematics (Science Domain International). 2017; 2(4):1-19.
DOI: 10.9734/ARJOM/2017/31306
18. Dillon B Schwalbach, Brian D Plourde, John P Abraham, Robert E Kohler. Drug dispersion for single- and multi-lumen catheters. Journal of Biomedical Science and Engineering. 2013;6:1021-1028.
19. Abraham JP, Gorman JM, Sparrow EM, Stark JR, Kohler RE. A mass transfer model of temporal drug deposition in artery walls. International Journal of Heat and Mass Transfer 2013;58:632–638.
20. John R Stark, John M Gorman, Ephraim M Sparrow, John P Abraham, Rob E Kohler. Controlling the rate of penetration of a therapeutic drug into the wall of an artery by means of a pressurized balloon. Journal of Biomedical Science and Engineering. 2013;6:527-532.
21. Noel M Naughton, Brian D Plourde, John R Stark, Simona Hodis, John P Abraham. Impacts of waveforms on the fluid flow, wall shear stress, and flow distribution in cerebral aneurysms and the development of a universal reduced pressure. Journal of Biomedical Science and Engineering. 2014;7:7-14.
22. Sun BY, Vallez LJ, Plourde BD, Abraham, JP, Stark JR. Influence of supporting tissue on the deformation and compliance of healthy and diseased arteries. Journal of Biomedical Science and Engineering. 2015;8:490-499.
Available:http://dx.doi.org/10.4236/jbise.2015.88046
23. Bestman AR. Global Models for the Biomechanics of Green Plants, Part 1. International Journal of Energy Research. 1991;16:677–684.

APPENDICES

$$d_1 = \frac{1}{I_o\left(\zeta_8^{1/2}\right)}\left[\Theta_w - \frac{I_o\left(\zeta_8^{1/2}r\right)}{2}\zeta_8^{1/2}c_1\frac{I_1\left(\zeta_6^{1/2}\right)}{\zeta_6^{1/2}}\right]$$

$$c_1 = \frac{1}{I_o\left(\zeta_6^{1/2}\right)}\left[\Theta_w - \frac{I_o\left(\zeta_6^{1/2}\right)}{2}\zeta_6^{1/2}b_1\frac{J_1\left(\zeta_4^{1/2}\right)}{\zeta_4^{1/2}}\right]$$

$$b_1 = \frac{1}{J_o\left(\zeta_4^{1/2}\right)}\left[\Theta_w - J_o\left(\zeta_4^{1/2}\right)\zeta_4^{1/2}a_1\frac{J_1\left(\zeta_2^{1/2}\right)}{\zeta_2^{1/2}}\right]$$

$$a_1 = \frac{1}{J_o\left(\zeta_2^{1/2}\right)}\left[\Theta_w - J_o\left(\zeta_2^{1/2}\right)\frac{\pi\zeta_2^{1/2}}{2}\gamma\Re\varepsilon Pe_h\aleph\right]$$

$$v_1 = -\frac{1}{I_o(M_1)}\left\{-M_1I_o(M_1)\left[-\frac{\Re\aleph}{2} + Grd_1\frac{I_1(\zeta_8^{1/2})}{\zeta_6^{1/2}} + -\frac{1}{20} - \frac{\zeta_6}{114} + M_1^2\left(\frac{1}{16} + \frac{\zeta_6}{192}\right)\right]\right.$$

$$\left. + \left(-\frac{M_1}{2} + \frac{M_1^2}{4}\right)\left[\frac{\Re\aleph I_1(M_1)}{M_1} - 2Grd_1\left(\frac{I_1(\zeta_8^{1/2})}{\zeta_8^{1/2}} - \frac{M_1^2}{6} - \frac{M_1^2\zeta_8}{40}\right) + \frac{1}{6} + \frac{\zeta_6}{80} + M_1^2\left(\frac{r^4}{16} + \frac{\zeta_6 r^6}{192}\right)\right]\right\}$$

$$k_1 = \frac{1}{I_o\left(\zeta_{16}^{1/2}\Re\alpha x\right)}\left[\gamma_1\Theta_w - \frac{I_o\left(\zeta_{16}^{1/2}\Re\alpha x\right)}{2}\zeta_{16}^{1/2}g_1\Re\alpha x\frac{I_o\left(\zeta_{14}^{1/2}\Re\alpha x\right)}{\zeta_{14}^{1/2}}\right]$$

$$g_1 = \frac{1}{I_o\left(\zeta_{14}^{1/2}\Re\alpha x\right)}\left[\gamma_1\Theta_w - \frac{I_o\left(\zeta_{14}^{1/2}\Re\alpha x\right)}{2}\zeta_{14}^{1/2}f_1\Re\alpha x\frac{J_1\left(\zeta_{12}^{1/2}\Re\alpha x\right)}{\zeta_{12}^{1/2}}\right]$$

$$f_1 = \frac{1}{J_o\left(\zeta_{12}^{1/2}\Re\alpha x\right)}\left[\gamma_1\Theta_w - \frac{J_o\left(\zeta_{12}^{1/2}\Re\alpha x\right)}{2}\pi\zeta_{12}^{1/2}e_1\Re\alpha x\frac{J_1\left(\zeta_{10}^{1/2}\Re\alpha x\right)}{\zeta_{10}^{1/2}}\right]$$

$$e_1 = \frac{1}{J_o\left(\zeta_{10}^{1/2}\Re\alpha x\right)}\left[\gamma_1\Theta_w - \frac{J_o\left(\zeta_{10}^{1/2}\Re\alpha x\right)}{2}\pi\zeta_{10}^{1/2}\left[-\gamma^2\Re^2\varepsilon^2Pe_h\left(\aleph + \aleph_1 x\right)\frac{\left(\Re\alpha x\right)^2}{2}\right.\right.$$

$$\left.\left. + 2\gamma^2\Re^2\varepsilon^2d_1\Re\alpha x\frac{I_1\left(\zeta_6^{1/2}\Re\alpha x\right)}{\zeta_6^{1/2}}\right]\right]$$

$$v_2 = -\frac{1}{I_o(M_1\Re\alpha x)}\left\{-M_1\Re\alpha xI_o(M_1\Re\alpha x)\left\{-\frac{\Re\aleph_1 x(\Re\alpha x)}{2} + Gc\left[\frac{k_1I_1(\zeta_{16}^{1/2}\Re\alpha x)}{\zeta_{16}^{1/2}} + \right.\right.\right.$$

$$\zeta_{16}^{1/2} g_1\left(\frac{(\Re\alpha x) I_1(\zeta_{16}^{1/2}\Re\alpha x)}{\zeta_{16}^{1/2}} + \frac{\zeta_{14}(\Re\alpha x)^4}{64} + \frac{\zeta_{14}\zeta_{16}(\Re\alpha x)^6}{384}\right)\Bigg] + \frac{M_1^2}{4}\Bigg[\frac{\Re\aleph_1(\Re\alpha x)^3}{3}$$

$$-2Gc\Bigg[k_1\left(\frac{(\Re\alpha x)^3}{3} + \frac{\zeta_{16}(\Re\alpha x)^5}{20}\right) + \zeta_{16}^{1/2} G_1\left(\frac{(\Re\alpha x) I_1(\zeta_{16}^{1/2}\Re\alpha x)}{2\zeta_{16}^{1/2}} +$$

$$\frac{\zeta_{14}(\Re\alpha x)^4}{64} + \frac{\zeta_{14}\zeta_{16}(\Re\alpha x)^6}{384}\right)\Bigg]\Bigg]\Bigg\} + \left(-\frac{M_1\Re\alpha x}{3} + \frac{M_1^3(\Re\alpha x)^3}{4}\right)\Bigg\{-\frac{\Re\aleph_1 x I_1(M_1\Re\alpha x)}{M_1}$$

$$-2Gc\Bigg[k_1\left(\frac{I_1(M_1\Re\alpha x)}{M_1} + \frac{\zeta_{16}(\Re\alpha x)^4}{16} + \frac{M_1^2\zeta_{16}(\Re\alpha x)^5}{80}\right) +$$

$$\zeta_{16}^{1/2} g_1\left(\frac{(\Re\alpha x) I_1(M_1\Re\alpha x)}{2M_1} + \frac{\zeta_{14}(\Re\alpha x)^4}{64} + \frac{\zeta_{14}M_1(\Re\alpha x)^6}{384}\right) + \frac{\zeta_{16}(\Re\alpha x)^4}{32} + \frac{\zeta_{16}M_1^2(\Re\alpha x)^6}{192} +$$

$$\frac{\zeta_{14}\zeta_{16}(\Re\alpha x)^6}{384} + \frac{\zeta_{14}\zeta_{16}M_1^2(\Re\alpha x)^8}{2048}\Bigg]\Bigg\}\Bigg\}$$

$$\zeta_2 = \sqrt{\Bigg\{\frac{1}{2}\Big(-\Big(-M_1^2 + 2N^2M_1^2 + 2M_1^2 - N^2\delta_1^2 - M_1^4 - 2\gamma R\varepsilon\Big) +$$

$$\sqrt{\Big(\Big(-M_1^2 + 2N^2M_1^2 + 2M_1^2 - N^2\delta_1^2 - M_1^4 - 2\gamma R\varepsilon\Big)^2 + 4\Big(-M_1^2\delta_1^2\gamma\Re\varepsilon + \gamma^2\Re^2\varepsilon^2\Big)\Big)}\Bigg\}$$

$$\zeta_4 = \sqrt{\Bigg\{\frac{1}{2}\Big(-\Big(-M_1^2 + 2N^2M_1^2 + 2M_1^2 - N^2\delta_1^2 - M_1^4 - 2\gamma R\varepsilon\Big) -$$

$$\sqrt{\Big(\Big(-M_1^2 + 2N^2M_1^2 + 2M_1^2 - N^2\delta_1^2 - M_1^4 - 2\gamma R\varepsilon\Big)^2 + 4\Big(-M_1^2\delta_1^2\gamma\Re\varepsilon + \gamma^2\Re^2\varepsilon^2\Big)\Big)}\Bigg\}$$

$$\zeta_6 = i\sqrt{\Bigg\{\frac{1}{2}\Big(-\Big(-M_1^2 + 2N^2M_1^2 + 2M_1^2 - N^2\delta_1^2 - M_1^4 - 2\gamma R\varepsilon\Big) +$$

$$\sqrt{\Big(\Big(-M_1^2 + 2N^2M_1^2 + 2M_1^2 - N^2\delta_1^2 - M_1^4 - 2\gamma R\varepsilon\Big)^2 + 4\Big(-M_1^2\delta_1^2\gamma\Re\varepsilon + \gamma^2\Re^2\varepsilon^2\Big)\Big)}\Bigg\}$$

$$\zeta_8 = i\sqrt{\Bigg\{\frac{1}{2}\Big(-\Big(-M_1^2 + 2N^2M_1^2 + 2M_1^2 - N^2\delta_1^2 - M_1^4 - 2\gamma R\varepsilon\Big) -$$

$$\sqrt{\Big(\Big(-M_1^2 + 2N^2M_1^2 + 2M_1^2 - N^2\delta_1^2 - M_1^4 - 2\gamma R\varepsilon\Big)^2 + 4\Big(-M_1^2\delta_1^2\gamma\Re\varepsilon + \gamma^2\Re^2\varepsilon^2\Big)\Big)}\Bigg\}$$

$$\zeta_{10} = \sqrt{\frac{1}{2}\{-\left(-\delta_1^2 M_1^2 - \left(N^2 - M^2\right)\left(\delta_1^2 - M^2\right) - M_1^2 N^2\right) +$$

$$\sqrt{\left(\left(-\delta_1^2 M_1^2 - \left(N^2 - M^2\right)\left(\delta_1^2 - M^2\right) - M_1^2 N^2\right)^2 - 4\left(\gamma\Re\varepsilon\left(M_1^2 N^2 \delta_1^2 - M_1^2 N^2 - M_1^2 \delta_1^2\right)\right)\right)}\}$$

$$\zeta_{12} = \sqrt{\frac{1}{2}\{-\left(-\delta_1^2 M_1^2 - \left(N^2 - M^2\right)\left(\delta_1^2 - M^2\right) - M_1^2 N^2\right) -$$

$$\sqrt{\left(\left(-\delta_1^2 M_1^2 - \left(N^2 - M^2\right)\left(\delta_1^2 - M^2\right) - M_1^2 N^2\right)^2 - 4\left(\gamma\Re\varepsilon\left(M_1^2 N^2 \delta_1^2 - M_1^2 N^2 - M_1^2 \delta_1^2\right)\right)\right)}\}$$

$$\zeta_{14} = i\sqrt{\sqrt{\frac{1}{2}\{-\left(-\delta_1^2 M_1^2 - \left(N^2 - M^2\right)\left(\delta_1^2 - M^2\right) - M_1^2 N^2\right) +$$

$$\sqrt{\left(\left(-\delta_1^2 M_1^2 - \left(N^2 - M^2\right)\left(\delta_1^2 - M^2\right) - M_1^2 N^2\right)^2 - 4\left(\gamma\Re\varepsilon\left(M_1^2 N^2 \delta_1^2 - M_1^2 N^2 - M_1^2 \delta_1^2\right)\right)\right)}\}$$

$$\zeta_{16} = i\sqrt{\sqrt{\frac{1}{2}\{-\left(-\delta_1^2 M_1^2 - \left(N^2 - M^2\right)\left(\delta_1^2 - M^2\right) - M_1^2 N^2\right) -$$

$$\sqrt{\left(\left(-\delta_1^2 M_1^2 - \left(N^2 - M^2\right)\left(\delta_1^2 - M^2\right) - M_1^2 N^2\right)^2}$$

Peer-review history:
The peer review history for this paper can be accessed here:
http://sciencedomain.org/review-history/20517